ISSN 1990-7931, Russian Journal of Physical Chemistry B, 2015, Vol. 9, No. 6, pp. 933–939. © Pleiades Publishing, Ltd., 2015.
Original Russian Text © V.Ya. Basevich, A.A. Belyaev, S.N. Medvedev, V.S. Posvyanskii, S.M. Frolov, 2015, published in Khimicheskaya Fizika, 2015, Vol. 34, No. 12, pp. 55–61.

COMBUSTION, EXPLOSION, AND SHOCK WAVES

Detailed Kinetic Mechanism of the Multistep Oxidation and Combustion of Isopentane and Isohexane

V. Ya. Basevich, A. A. Belyaev, S. N. Medvedev, V. S. Posvyanskii, and S. M. Frolov

Semenov Institute of Chemical Physics, Russian Academy of Sciences, ul. Kosygina 4, Moscow, 119991 Russia

e-mail: belyaev@center.chph.ras.ru

Received March 11, 2015

Abstract—A detailed kinetic mechanism was developed for the oxidation and combustion of isopentane (2-methylbutane) and isohexane (2-methylpentane), which describes both high-temperature reactions and a multistep process in the region of low temperatures. These hydrocarbons were chosen because they, together with isobutane, are the first members in the homologous series of isomerized alkanes and a higher member of this series—isooctane (2,2,4-trimethylpentane)—exhibited multistep self-ignition in experiments; in this case, the above isomers can be important intermediate products. The process of the multistep self-ignition of the above hydrocarbons under specific conditions occurs in three sequential steps (in the form of cold and blue flames and hot explosion) characteristic of normal alkanes. The calculations of self-ignition and flame propagation were performed by the developed mechanism; the results of the calculations were compared with the experimental data and their satisfactory qualitative and quantitative agreement was obtained.

Keywords: isopentane, isohexane, motor fuel, kinetic mechanisms, self-ignition, multistep process, flame propagation

DOI: 10.1134/S1990793115060159

INTRODUCTION

Based on the survey of a large body of experimental data, Sokolik [1] made a generalization and introduced a concept of the multistep self-ignition of hydrocarbons with the separate steps of cold and blue flames and hot explosion. This multistep process was observed in experiments on the oxidation of many hydrocarbons [1, 2]. Detailed kinetic mechanisms were proposed in the literature for the oxidation and combustion of different hydrocarbons, both normal and isomerized, including those considered here (for example, see refs. [3–5]). However, none of the well-known publications indicates that these mechanisms adequately describe multistep self-ignition with the above three stages. The only exception is a publication by Machrafi and Cavadias [6], who considered the phenomenology of the self-ignition of standard fuels (*n*-heptane and isooctane). They referred to the blue flame as preignition and proposed a complex kinetic explanation for it through reactions with aromatic structures, which cannot be applied to individual normal-structure hydrocarbons and their isomers.

Previously, we proposed a kinetic explanation for the appearance of the blue flame, which is applicable to normal alkanes up to cetane [7] and to isobutane [8]. The aim of this work was to develop a detailed kinetic mechanism for isopentane *i*-C_5H_{12} (2-methylbutane) and isohexane *i*-C_6H_{14} (2-methylpentane (2MP)) in order to adequately describe not only high-temperature reactions but also multistep oxidation and combustion reactions in the region of low temperatures, as this was made earlier for isobutane. Supposedly, these hydrocarbons are intermediate products in the oxidation of isooctane—one of the reference individual hydrocarbons that simulate the behavior of real motor fuels in conventional engines and in the combustion chambers of direct-flow jet engines with controlled detonation combustion [9]. Another important aspect of the study of isomerized hydrocarbons is related to the problem of the antiknock value of motor fuels in conventional engines: gasoline can contain to a third of isoparaffins.

MECHANISM CONSTRUCTION

It is well known that there is much in common between the phenomenology of the oxidation and the combustion of hydrocarbons [4]. For constructing a detailed kinetic multistep mechanism of the oxidation and combustion of *i*-C_5H_{12} and *i*-C_6H_{14}, we used a procedure of analogies with the selection of reactions important for the multistep process; this procedure worked very well in the examination of normal alkanes and isobutane. The detailed kinetic mechanism of normal octane oxidation, which included elementary reactions for normal pentane and hexane, and the detailed kinetic mechanism of isobutane oxidation were taken as the basis, and the principle of a nonextensive construction of mechanisms was used. This

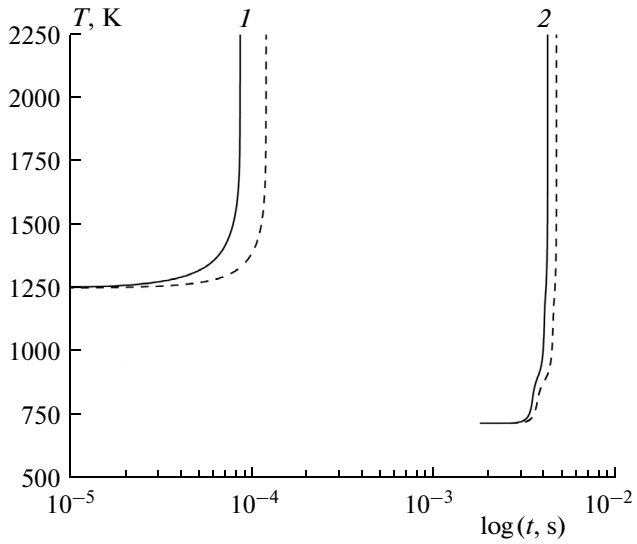

Fig. 1. Calculated time dependences of temperature in the self-ignition of the stoichiometric air mixtures of (dashed lines) i-C_5H_{12} and (solid lines) i-C_6H_{14}. Initial temperatures T_0 = (*1*) 1250 and (*2*) 714 K; initial pressure P = 36 atm (abs.).

principle is based on the assumption that low-temperature branching is related to a group of reactions with one oxygen addition (to the linear part of a molecule) and a limited number of additional components—one main isomerized component corresponds to each normal-structure component and represents the entire group of particles with different structures but a given empirical formula.

For obtaining a new mechanism, 18 isomerized components (i-C_5H_{12}, i-C_5H_{11}, i-$C_5H_{11}O_2$, i-$C_5H_{11}O_2H$, i-$C_5H_{11}O$, i-C_4H_9CHO, i-C_4H_9CO, i-C_5H_{10}, i-C_5H_9, i-C_6H_{14}, i-C_6H_{13}, i-$C_6H_{13}O_2$, i-$C_6H_{13}O_2H$, i-$C_6H_{13}O$, i-$C_5H_{11}CHO$, i-$C_5H_{11}CO$, i-C_6H_{12}, and i-C_6H_{11}) and 1078 reactions analogous to those of isobutene were added to the constituents of the above detailed kinetic mechanisms. The thermochemical parameters of the components—the enthalpy $\Delta H^\circ_{f\,298}$, the entropy S^0_{298}, and the coefficients c_0, c_1, c_2, c_3, and c_4 in the formula of heat capacity at constant pressure $c_p = c_0 + c_1T/10^3 + c_2T^2/10^6 + c_3T^3/10^9 + c_4T^4/10^{12}$—were calculated based on the well-known recommendations and additivity rules for two temperature ranges (low-temperature and high-temperature ranges). Finally, the mechanism included 126 components and 1487 pairs of reactions (each reaction proceeds in the forward and opposite directions).

The selection of the Arrhenius parameters of reaction rate constants is very difficult to perform because the experimental data are insufficient. Therefore, the kinetic parameters were calculated in accordance with a published procedure [8] based on a set of the rate constants of reactions with the participation of normal-structure components using the two-parameter form of a rate constant with the preexponential factor A and the activation energy E:

$$A_{i(i)} = A_{i(n)}\exp[(\Delta S_{i(i)} - \Delta S_{i(n)})/R],$$

$$E_{i(i)} = E_{i(n)} - 0.25[\Delta H_{i(i)} - \Delta H_{i(n)}]$$

for exothermic reactions;

$$E_{i(i)} = E_{i(n)} + 0.75[\Delta H_{i(i)} - \Delta H_{i(n)}]$$

for endothermic reactions,

where $A_{i(i)}$ and $A_{i(n)}$ are the preexponential factors of the rate of the ith reaction with the participation of (i) isomerized and (n) normal-structure components, respectively; $E_{i(i)}$ and $E_{i(n)}$ are the activation energies of the ith reaction with the participation of (i) isomerized and (n) normal-structure components, respectively; T is temperature; R is the gas constant; $\Delta S_{i(i)}$ and $\Delta S_{i(n)}$ are the corresponding changes in the entropy of reactions; and $\Delta H_{i(i)}$ and $\Delta H_{i(n)}$ are the corresponding changes in the enthalpy of reactions. As in our previous works [7, 8], the Arrhenius parameters thus obtained were corrected for a limited number of reactions (less than ten). A file with the kinetic mechanism data will be placed in the Internet at www.combex.ru.

MECHANISM TESTING

Self-Ignition of Gas Mixtures

The detailed kinetic mechanism developed was tested by comparing the calculated process parameters of i-C_5H_{12} and i-C_6H_{14} self-ignition with the experimental data. The standard kinetic program developed by M.G. Neigauz at the Semenov Institute of Chemical Physics, Russian Academy of Sciences was used for the calculations of self-ignition at a constant pressure. The calculations were conducted in the following ranges of initial temperatures and pressures: $T_0 = 550$–1850 K and $P = 1$–36 atm (abs.). The composition of the mixtures varied from strongly depleted to strongly enriched in fuel with dilution by argon and nitrogen.

As an example, Fig. 1 shows the typical calculated time dependences of temperature for the self-ignition of the stoichiometric mixtures of i-C_5H_{12} and i-C_6H_{14} with air, which are characteristic of high and low initial temperatures. At high temperatures above 1000 K, the self-ignition occurs as a single-step process. At a relatively low temperature (here, 714 K), the self-ignition appears like a two-step process, although it is actually a multistep process at this and lower temperatures (Fig. 2). The first stepwise temperature increase in the self-ignition of i-C_5H_{12} (Fig. 2a) at $T_0 = 714$ K occurs at the point in time $t \sim 3.6$ ms due to the appearance of cold flame. After ~4.5 ms, blue flame appears, and then hot explosion occurs at ~4.8 ms. Thus, the multistep self-ignition process manifests itself as the sequential appearance of cold and blue flames and hot explosion. The acceleration of reaction in the cold flame is a consequence of branching upon the decay of the alkyl hydroperoxide i-$C_5H_{11}O_2H$ with the forma-

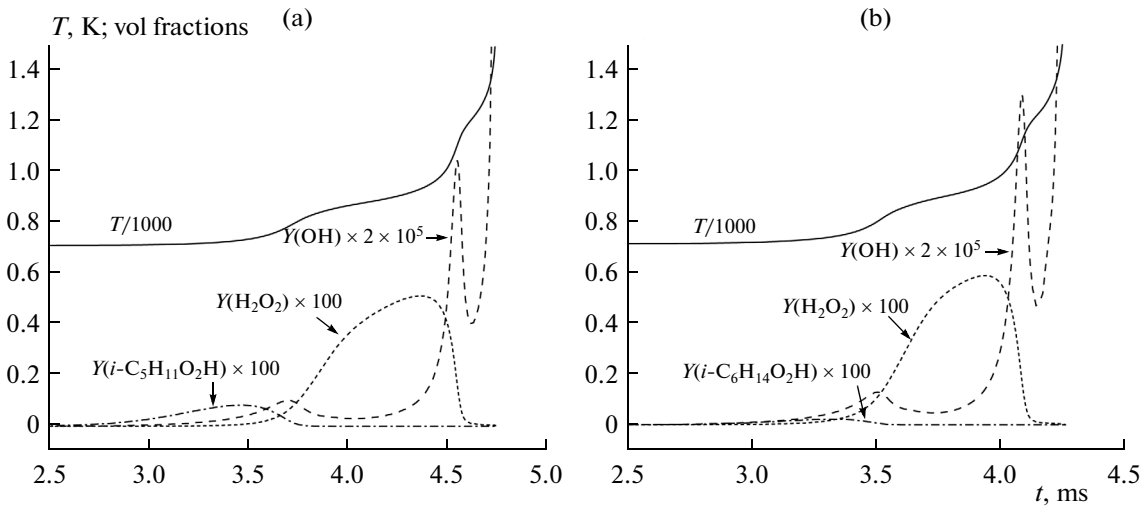

Fig. 2. Calculated time dependences of temperature and the concentrations of hydroxyl, alkyl hydroperoxide, and hydrogen peroxide in the self-ignition of the stoichiometric air mixtures of (a) i-C_5H_{12} and (b) i-C_6H_{14}. Initial pressure $P = 36$ atm (abs.); initial temperature $T_0 = 714$ K.

tion of hydroxyl and oxy radicals. The appearance of blue flame is caused by branching because of the degradation of hydrogen peroxide H_2O_2. This is clearly indicated by the behavior of calculated curves for peroxide concentrations and the occurrence of two peaks in the curve of hydroxyl concentration. Although this clear separation of steps not always manifests itself in the experiments because of temperature heterogeneities, it locally occurs in actual practice. The process of the self-ignition of i-C_6H_{14} proceeds analogously (Fig. 2b).

Figure 3 compares the calculated (curves) and measured (points [5]) delays of the self-ignition of the stoichiometric air mixtures of i-C_5H_{12} at different temperatures; in this case, the comparison was carried out based on the delays of cold flame and hot explosion. Note that Ribaucour et al. [5] did not specify pressure in the process of self-ignition. Therefore, in the calculation, the pressure was taken to be constant and equal to $P_0 = 11$ atm, which corresponded to the pressure of the end of compression. Heat losses were not considered in the calculation.

Figure 4 compares the calculated (curves) and measured (points [4]) delays of the self-ignition of the stoichiometric mixtures of i-C_5H_{12}–O_2–Ar at an oxygen concentration of 21%, the pressure $P_0 = 1$ atm, and different temperatures. Figure 5a shows experimental data [4] on the concentration of hydroxyl for a mixture containing 0.1% i-C_5H_{12} and 0.8% O_2 in Ar at $T_0 = 1606$ K and the pressure $P = 1.68$ atm, and Fig. 5b shows the calculated curve for the concentration of hydroxyl.

Earlier, Burcat et al. [3] reported experimental data on the parameter β proposed by them for describing the self-ignition delays t_i of isohexane i-C_6H_{14}:

$$\log\beta = \log\{t_i/([2MP]^{0.69}[O_2]^{-1.27}[Ar]^{0.38})\},$$

where [2MP], [O_2], and [Ar] are the concentrations of isohexane, oxygen, and argon, respectively. The experiments were carried out with different mixtures at different pressures and temperatures. Figure 6 compares the measured parameter β (Fig. 6a) and the parameter calculated for the same conditions as those used in the experiments (Fig. 6b). In both of the figures, a solid line corresponds to the experimental root-mean-square values of logβ. The agreement between

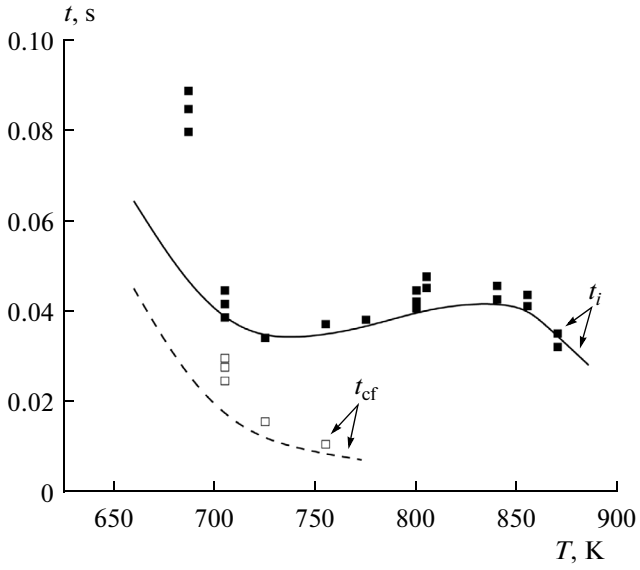

Fig. 3. Comparison between the (curves) calculated and (points [5]) measured temperature dependences of the delays of ignition in the stoichiometric air mixtures of i-C_5H_{12}: t_{cf} and t_i are the delays of cold flame and hot explosion, respectively. Pressure $P = 11$ atm (abs.).

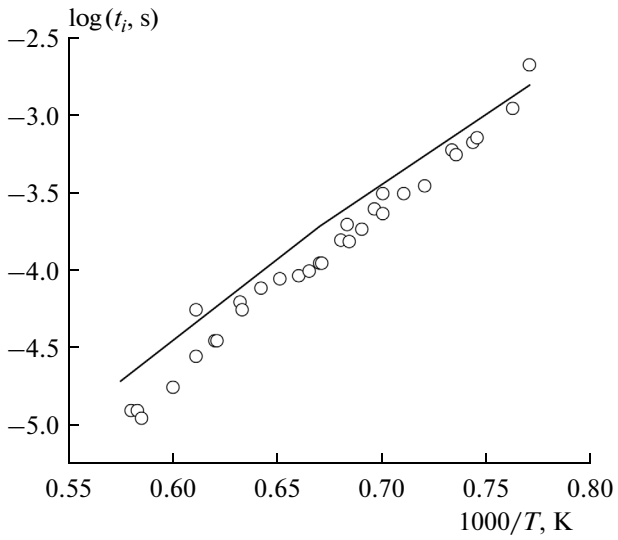

Fig. 4. Comparison between the (curves) calculated and (points [4]) measured temperature dependences of the delays of ignition in the stoichiometric mixtures of i-C_5H_{12}–O_2–Ar. Oxygen concentration, 21%; pressure $P = 1$ atm (abs.).

the experimental and calculated data obtained in Figs. 3–6 seems satisfactory.

Laminar Flame Propagation

Additionally, we performed calculations to determine the velocity of laminar flame propagation u_n in the mixtures of i-C_5H_{12} and i-C_6H_{14} with air depending on the fuel excess coefficient f. The calculation procedure was described in detail elsewhere [10].

Figure 7 compares the calculated (curve) and experimental (points) values of u_n for the air mixtures of i-C_5H_{12} at different pressures and temperatures. Gerstein et al. [13] measured the value of $u_n = 36.8$ cm/s for an air mixture of i-C_6H_{14} at $f = 1.15$ and normal initial conditions, whereas the value calculated for these conditions is 32.5 cm/s.

Figure 8 compares the calculated (curve) and experimental (points [14]) dependences of u_n on the fuel excess coefficient f for the air mixtures of i-C_6H_{14} at an initial temperature of 680 K and an initial pressure of 18.5 atm.

In general, taking into account possible measurement errors and the approximate values of the constants of reactions in the developed detailed kinetic mechanism, we can consider that the experimental and calculated data are in satisfactory agreement. Note that it is possible to attain very good agreement with particular experimental data by varying the constants of some reactions (within the limits of their uncertainty); however, in this work, we carried out calculations with the use of the fixed values of the kinetic parameters of all elementary reactions that enter into the detailed kinetic mechanism.

Compression Ignition under the Conditions of an Internal Combustion Engine

Antiknock quality is an important physicochemical property of hydrocarbons, which manifests itself on compression ignition under the conditions of an internal combustion engine. Computational programs (for

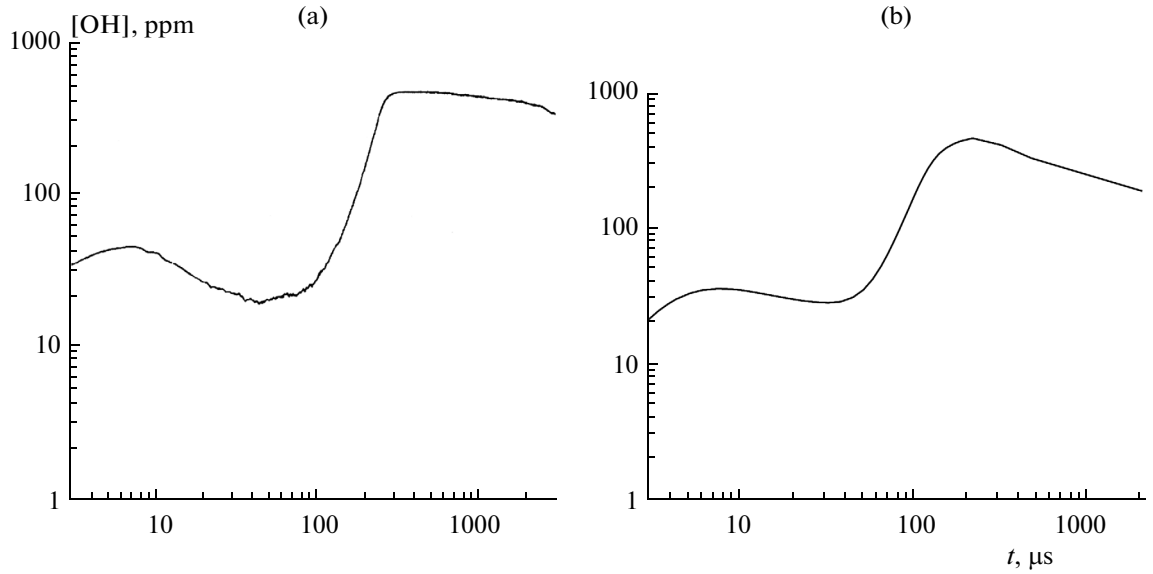

Fig. 5. Time dependences of hydroxyl concentration in the self-ignition of a mixture of 0.1% i-C_5H_{12}–0.8% O_2–Ar at $T_0 = 1606$ K and $P = 1.68$ atm (abs.): (a) experimental data [4] (solid line) and (b) calculated data.

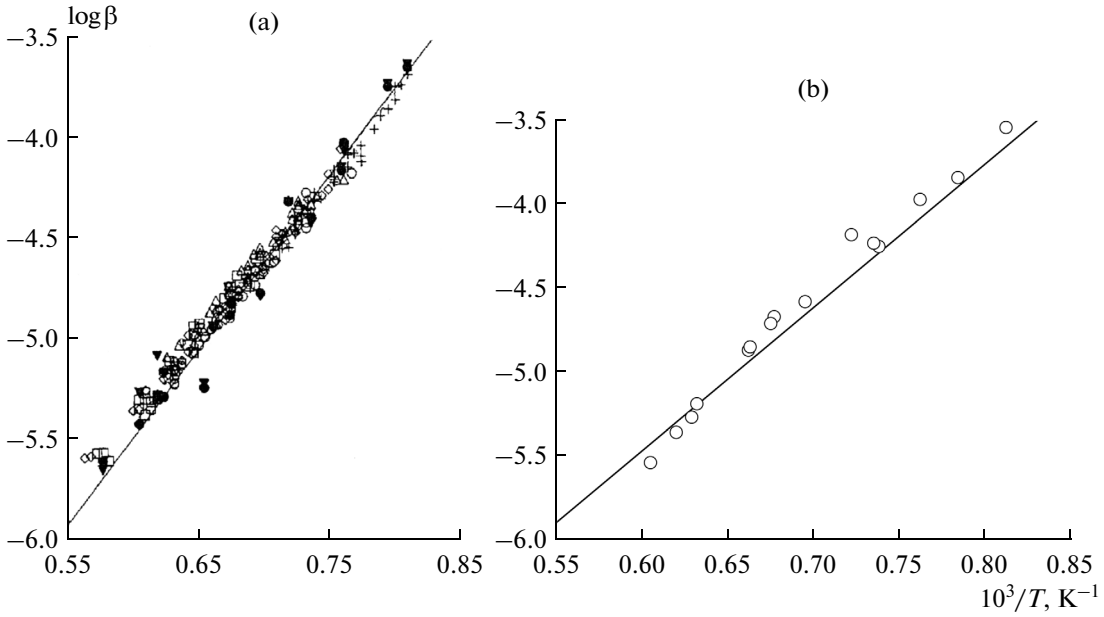

Fig. 6. Comparison between the (a) measured [3] and (b) calculated dependences of the parameter β for the delays of ignition in the mixtures of i-C_6H_{14}–O_2–Ar. Concentrations of i-C_6H_{14} – 0.5–2.0%; concentrations of O_2, 4.75–19.3%; temperature T_0 = 1231–1651 K; and pressure P = 2.82–4.069 atm (abs.).

example, see [15, 16]), make it possible to approximately calculate the fundamental characteristic of the antiknock properties of hydrocarbons—their ignition quality. For this purpose, a so-called indicator diagram is constructed as the dependence of engine cylinder pressure on crank angle upon the displacement of a piston. Figure 9 gives an example of such a calculation diagram with self-ignition; additionally, it shows the dependence of temperature on crank angle. The calculation represented in Fig. 9 was carried out without taking into account the heat exchange of gases with the cylinder walls of the internal combustion engine.

The compression of a charged homogeneous fuel–air mixture begins in the position of a piston at the bottom dead center and a maximum cylinder capacity (a crank angle of −180°) and ends at the top dead center at a crank angle of 0°. In an example shown in Fig. 9 at the engine speed n = 600 min^{-1}, the time of charge compression is t = 50 ms (a crank angle of 1° corresponds to a time of ~0.278 ms), and the compression ratio is ε = 13 (a ratio of the initial maximum volume of a mixture to the minimum volume at the upper position of a piston). It is evident that self-ignition comes into play before the bottom dead center (with the manifestation of a multistep process) followed by the combustion of a charge with expansion (pressure and temperature maximums at a crank angle of about ~−4°).

Figure 10 shows the dependences of temperature on crank angle for the air mixtures of i-C_5H_{12}, i-C_6H_{14}, n-C_5H_{12}, and n-C_6H_{14}. It is evident that the antiknock quality of isomerized hydrocarbons is higher than that of normal hydrocarbons. In actual practice, the antiknock rating of fuel is evaluated according to a special procedure by a so-called octane number: the greater the octane number, the longer the delay of firing. According to reference data, the octane numbers of n-C_6H_{14} and n-C_5H_{12} are 25 and 61, and

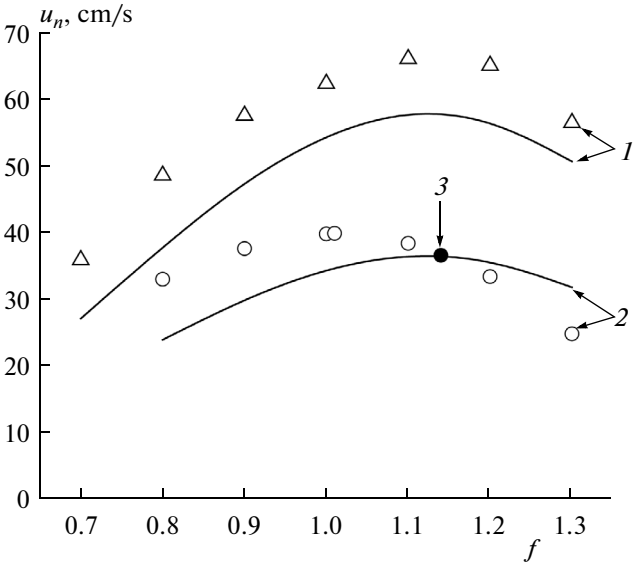

Fig. 7. Comparison between the (curves) calculated and (points) measured dependences of the velocity of laminar flame propagation u_n on the fuel excess coefficient f for the air mixtures of i-C_5H_{12} and i-C_6H_{14} (curve *1* and △ [11]) at the pressure P = 3.04 atm (abs.) and the initial temperature T_0 = 450 K and (curve *2*, ○ [12] for i-C_5H_{12}, point *3* from [13] for i-C_6H_{14}) at atmospheric pressure and the initial temperature T_0 = 298 K.

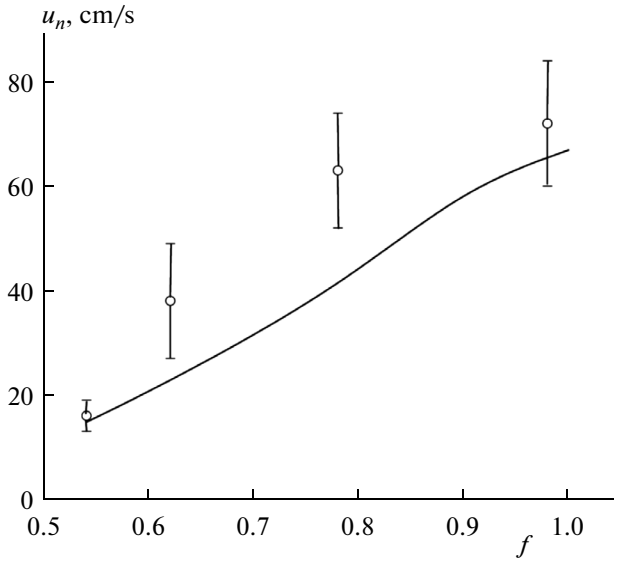

Fig. 8. Comparison between the (curve) calculated and (points [14]) measured dependences of the velocity of laminar flame propagation u_n on the fuel excess coefficient f for an air mixture of i-C_6H_{14} at the pressure $P = 18.5$ atm (abs.) and the initial temperature $T_0 = 680$ K.

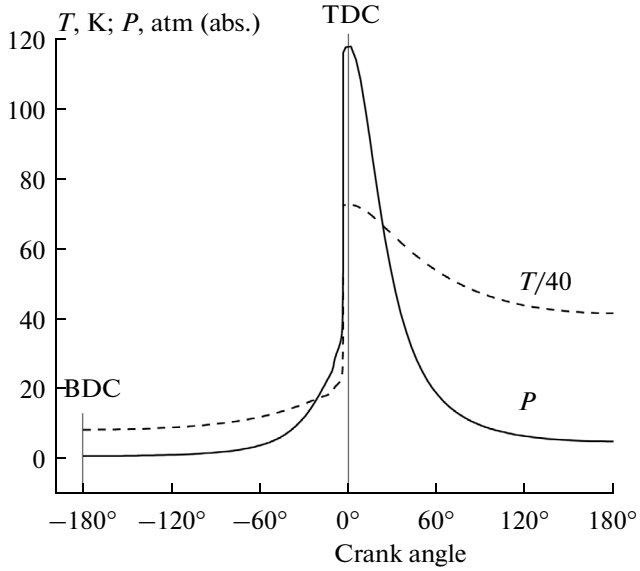

Fig. 9. Calculated indicator diagram and the calculated dependence of temperature on crank angle for a stoichiometric air mixture of i-C_5H_{12} in an internal combustion engine. Initial pressure $P_0 = 1$ atm (abs.); initial temperature $T_0 = 340$ K; compression ratio $\varepsilon = 13$; and number of revolutions $n = 600$ min^{-1}.

those of i-C_6H_{14} and i-C_5H_{12} are 73 and 81, respectively. Thus, the diagrams indicate a qualitative agreement between the calculated and experimental data.

CONCLUSIONS

The above comparisons between the calculated and experimental data on the delays of ignition and the velocity of laminar flame propagation allowed us to conclude that the detailed kinetic mechanism developed for the oxidation and combustion of isopentane and isohexane, in general, correctly reflects all basic laws governing the process. Therefore, the application of the principle of a nonextensive construction of kinetic mechanisms is generally reasonable. The most important special feature of the detailed kinetic mech-

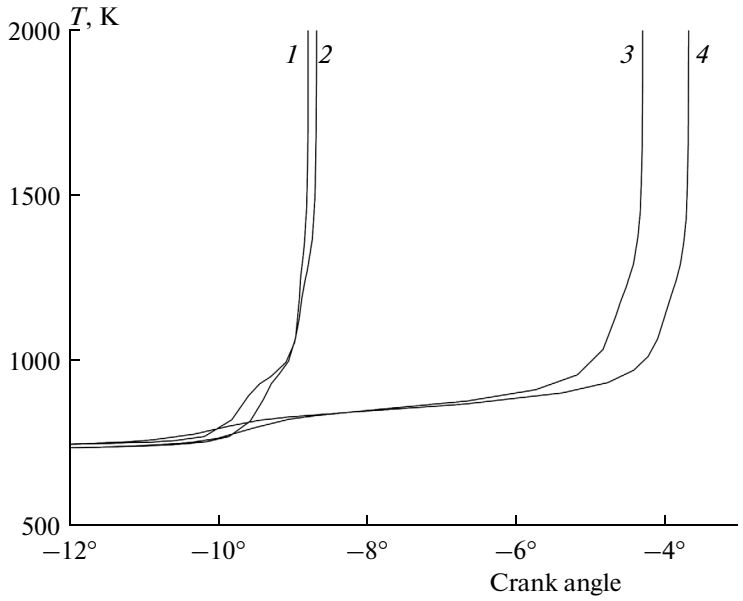

Fig. 10. Calculated dependence of the temperature T on the crank angle for the stoichiometric air mixtures of n-C_6H_{14} (*1*), n-C_5H_{12} (*2*), i-C_6H_{14} (*3*), and i-C_5H_{12} (*4*). Compression ratio $\varepsilon = 13$; $P_0 = 1$ atm (abs.); $T_0 = 340$ K; and $n = 600$ min^{-1}.

anism developed is that it describes a multistep process in the form of cold and blue flames and hot explosion on low-temperature self-ignition, which was detected experimentally.

ACKNOWLEDGMENTS

This work was supported in part by the Ministry of Education and Science of the Russian Federation within the framework of the Federal Target-Oriented Program "Research and Development in the Priority Directions of Russia's Scientific and Technological Complex for 2014–2020" (state contract no. 14.609.21.0001; contract identifier: RFMEFI57914X0038), the Russian Foundation for Basic Research (grant no. 15-08-00782), and the Russian Science Foundation (project no. 14-13-00082).

REFERENCES

1. A. S. Sokolik, *Self-Ignition, Flame and Detonation in Gases* (Akad. Nauk SSSR, Moscow, 1960) [in Russian].
2. D. Downs, J. S. Street, and R. W. Wheeler, Fuel **32**, 270 (1953).
3. A. Burcat, E. Olchanski, and C. Sokolinski, Combust. Sci. Technol. **147**, 1 (1999).
4. M. A. Oehlschlaeger, D. F. Davidson, J. T. Herbon, and R. K. Hanson, Int. J. Chem. Kinet. **36**, 67 (2004).
5. M. Ribaucour, R. Minetti, L. R. Sochet, et al., Proc. Combust. Inst. **28**, 1671 (2000).
6. H. Machrafi and S. Cavadias, Combust. Flame **155**, 557 (2008).
7. V. Ya. Basevich, A. A. Belyaev, V. S. Posvyanskii, and S. M. Frolov, Russ. J. Phys. Chem. B **7**, 161 (2013).
8. V. Ya. Basevich, A. A. Belyaev, S. N. Medvedev, V. S. Posvyanskii, and S. M. Frolov, Russ. J. Phys. Chem. B **9**, 268 (2015).
9. S. M. Frolov, A. E. Barykin, and A. A. Borisov, Khim. Fiz. **23** (3), 17 (2004).
10. A. A. Belyaev and V. S. Posvyanskii, Algoritmy Programmy, Inform. Byull. Gos. Fonda Algoritm. Progr. SSSR, No. 3, 35 (1985).
11. J. T. Farrell, R. J. Johnston, and I. P. Androulakis, SAE Paper No. 2004-01-2936 (Society of Automotive Engineers, 2004), pp. 1–22.
12. G. I. Gibbs and H. F. Calcote, J. Chem. Eng. Data **4**, 226 (1959).
13. M. Gerstein, O. Levine, and E. L. Wong, J. Am. Chem. Soc. **73**, pp. 418–422 (1951).
14. M. P. Halsted, D. B. Pye, and C. P. Quinn, Combust. Flame **22**, 89 (1974).
15. V. Ya. Basevich, A. A. Belyaev, A. N. Gots, V. S. Posvyanskii, I. V. Semenov, S. M. Frolov, and F. S. Frolov, Goren, Vzryv **5** (5), 167 (2012).
16. CHEMKIN-PRO Release 15083 (17.04.2009).

Translated by V. Makhlyarchuk